PERFORMANCE ANALYSIS OF OPTICAL BURST SWITCHED NETWORKS WITH LIMITED-RANGE WAVELENGTH CONVERSION, RETRANSMISSION AND BURST SEGMENTATION

Tuan Phung-Duc   Hiroyuki Masuyama   Shoji Kasahara   Yutaka Takahashi
Kyoto University

Abstract   This paper considers the performance of optical burst switched networks with burst segmentation, wavelength conversion and upper-layer retransmission. When a burst arrives at an intermediate node and finds its allocated wavelength occupied, it attempts to find another idle wavelength among a limited number of wavelengths to which the allocated wavelength can be converted. If the incoming burst cannot find any idle wavelength in the range, the ongoing burst in the allocated wavelength is segmented and its tail part which overlaps with the incoming burst is dropped and retransmitted as a retransmitted burst in a later time by upper-layer retransmission mechanisms such as TCP. Focusing on an outgoing optical fiber shared under wavelength division multiplexing, we model it as a multi-server retrial queueing system without waiting room, in which an arriving customer chooses his server out of a group of servers with a state-dependent probability. We formulate a bivariate Markov chain to analyze the model and also perform simulation experiments to validate the analysis model. Numerical examples show that the wavelength conversion technique is effective to lessen the contention of bursts at low traffic intensity and that the degree of contention among bursts is almost insensitive to the retransmission rate. They further reveal that even a small range of wavelength conversion can significantly alleviate the contention among bursts.

Keywords: Queue, multiserver retrial queue, optical burst switched network, burst segmentation, upper-layer retransmission, limited-range wavelength conversion

1.   Introduction

Optical burst switching (OBS) is considered as one of the promising technologies for the next generation Internet over wavelength division multiplexing (WDM) networks [1, 3, 12, 13, 16, 17]. In OBS networks, multiple IP packets are aggregated into a burst at an OBS edge node, and the corresponding control packet is transmitted ahead of the burst in order to configure switching resources for the burst transmission. After some offset time, the burst is sent into the OBS network without receiving an acknowledgement (ACK) message. This may cause burst contention at an intermediate node, and hence the contention resolution is one of the most important issues for OBS networks.

Existing resolution schemes for burst contention are classified into burst-level resolution and packet-level resolution. The former includes deflection routing [4], wavelength conversion [14], and buffering with fiber delay line (FDL), while a typical scheme for the latter is burst segmentation [18, 19]. In burst segmentation, when contention occurs at an outgoing link of some intermediate OBS node, the overlapping part of either the burst already in transmission or the newly arriving one is discarded. Note that in the conventional OBS, the contending burst is entirely dropped when contention occurs.

The performance of the burst segmentation was extensively investigated in the litera-

ture. Vokkarane et al. [18] considered the burst segmentation with deflection, in which a segmented part of a burst is not discarded but rerouted to its destination with deflection routing. They evaluated the packet loss probability and the average output burst size by simulation. Vokkarane and Jue [19] analyzed the packet loss probability by comparing the average burst size at destination with that of the original bursts. In [6], optical composite burst switching (OCBS) with head-dropping was proposed.

The wavelength conversion is a burst-contention avoidance technique in which a burst from an incoming wavelength is switched to a different outgoing wavelength. If the conversion range is limited, it is called a limited wavelength conversion technique. In [14], path blocking probabilities were evaluated with the link blocking probabilities obtained by the Erlang fixed-point approximation.

In terms of retransmission mechanism, the TCP throughput over OBS networks with burst-level retransmission was considered in [21], and Choi et al. [5] analyzed the burst blocking probability at an OBS node with buffering and retransmission mechanism at optical level. Note that the retransmission mechanism in [5, 21] works at OBS level, but not at upper layer. In our previous work [11], burst segmentation with upper-layer retransmission was studied. Focusing on a wavelength at an outgoing port of an OBS core node, we analyzed the wavelength utilization and the average output burst size using a single-server retrial queue without waiting room. To the best of our knowledge, the performance analysis of OBS networks equipped with limited range wavelength conversion, burst segmentation and retransmission, has not been studied yet.

In this paper, we consider the performance of the OBS network with burst segmentation, wavelength conversion and upper-layer retransmission. We develop a new multiserver retrial queueing model with random server selection for the OBS network. In this queueing model, each arriving customer can receive service from only a group of servers. If there are no idle servers for the arriving customer, an existing customer is preempted and it returns to a virtual waiting line called "orbit" and attempts for the rest of its service after some time. Since each dropped part due to burst segmentation is retransmitted at a later time and each burst can be transmitted by a group of wavelengths to which the allocated wavelength can be converted, we model the OBS network by the multiserver retrial queueing model. We analyze the queueing system by a continuous-time bivariate Markov chain to derive the average number of busy wavelengths at the outgoing port, the average number of retransmitted bursts, the contention probability and the average output burst size. Note that our model can describe no-wavelength conversion, limited-range wavelength conversion and full-range wavelength conversion as its special cases. The model for the full-range wavelength conversion case is identical to the conventional multi-server retrial queueing model whose details are presented in [7].

The rest of this paper is organized as follows. Section 2 describes the OBS network with burst segmentation and wavelength conversion. Section 3 presents the analysis model for burst segmentation with upper-layer retransmission in OBS networks with and without wavelength conversion. The analysis of the model is presented in Section 4. Some numerical examples are shown in Section 5, and finally conclusions are presented in Section 6.

2. OBS Network and Burst Segmentation

In this section, we briefly summarize how the OBS network equipped with burst segmentation and limited wavelength conversion works for preventing burst contention.

2.1.   OBS network with wavelength conversion

An OBS network consists of a set of edge and core OBS nodes. In the OBS network, a burst is assembled with multiple IP packets at an ingress-edge node, and then is transmitted to its egress node with a control packet. The control packet is transmitted before the burst transmission, and it reserves a wavelength at each core node in order to transmit the burst. After some offset time, the burst is sent into the OBS network without receiving the positive acknowledgement from the control packet. The control packet includes the source and destination addresses of the burst. This may also include the length of the burst if it has been already assembled prior to sending the control packet. When the control packet fails to reserve a wavelength at a link of an intermediate node, the corresponding burst might contend with other bursts at that node. In this case, no NACK message is sent back to the ingress-edge node to inform about the contention of the burst. Instead, some contention resolution schemes implemented at the node might work to lessen the frequency of packet loss due to the contention. One of these schemes is burst segmentation which will be explained in detail in subsection 2.2.

The reserved wavelengths are released according to either explicit release or estimated release after the burst has been sent through [1]. In explicit release, the ingress-node sends another control signal to let OBS nodes know about the end of a burst transmission. In estimated release, OBS nodes know exactly the length of the burst from the control packet and therefore can calculate the time to release occupied wavelengths. For the details of the release of resources (OBS switches and wavelengths), the readers are referred to [1].

Since the burst is sent to the OBS network without receiving an ACK message, the burst may suffer from contention at an intermediate node due to congestion. In this paper, we consider the OBS network with wavelength conversion capability. When a burst arriving at an intermediate node of the OBS network finds the desired outgoing wavelength busy, the arriving burst is switched to a different outgoing wavelength. The wavelength conversion is classified into two categories: full-range wavelength conversion and limited-range wavelength conversion. In full-range wavelength conversion, a burst carried by incoming wavelength can be converted onto any of outgoing wavelengths, while a limited wavelength conversion, the selection of an outgoing wavelength has some constraint on its range. Note that full-range conversion is a special case of limited-range wavelength conversion.

2.2.   Burst segmentation

In conventional OBS networks, when burst contention occurs, only one of contending bursts is transmitted and the others are discarded. Since a burst is a collection of a large number of packets, even the loss of a single burst leads to the loss of a large amount of data. To overcome this weakness and to improve the throughput of packets, burst segmentation was firstly introduced in [18]. Each burst consists of multiple basic units called segments, each of which contains a single or multiple packets. Bursts can be segmented into groups of segments when contention for a common wavelength among them occurs, and only a single group of segments out of them are transmitted and the others are dropped.

There are two approaches for dropping burst segments: head dropping and tail dropping. In head dropping, the head part of the contending burst is discarded while in tail dropping, the tail part of the burst already in transmission is dropped. It has been reported in [18] and [19] that tail dropping is suitable for TCP because there is a better chance of in-sequence delivery of TCP segments at destination, resulting from TCP retransmission of dropped segments. This paper considers the tail dropping approach. (See Figure 1.) Under the tail-dropping segmentation, if the control packet does not find an available wavelength at
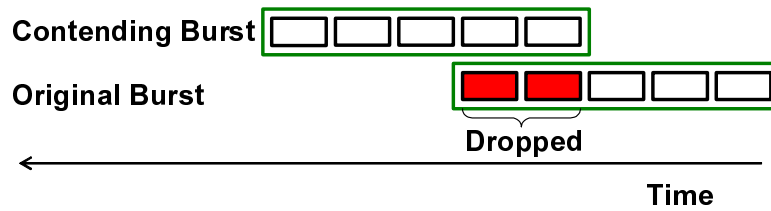
Figure 1: Tail-dropping burst segmentation

an intermediate node, the existing reservation by another burst is preempted by the control packet and the reservation is taken over by the corresponding burst, which will be forwarded to the next node.

3. Analysis Model

In this section, we describe a queueing model for OBS networks with burst segmentation, wavelength conversion and upper-layer retransmission.

3.1. Retrial queue with random server selection

We focus on an outgoing port of a core node in an OBS network with a limited range of wavelength conversion. There exist W wavelengths $(w_1, w_2, \ldots, w_W)$ in the outgoing port. A new burst arrives at the outgoing port according to a Poisson process with rate λ and its transmission time is exponentially distributed with rate μ.

In the OBS core node, when wavelength w_l $(l = 1, 2, \ldots, W)$ is in use, a burst carried by wavelength w_l is forwarded onto one of the other wavelengths chosen within in a certain limited range $\mathcal{W}_l$. When all the wavelengths in the range $\mathcal{W}_l$ are busy, the incoming burst interrupts the transmission of a burst over wavelength w_l and preempts the wavelength. Further the remaining part of the preempted burst is retransmitted after some time. In this paper, we assume that the conversion range $\mathcal{W}_l$ $(l = 1, 2, \ldots, W)$ for wavelength w_l is given by

$$\mathcal{W}_l = \{w_i; \max(1, l - d) \leq i \leq \min(l + d, W)\}, \tag{3.1}$$

where d $(d = 0, 1, \ldots, W - 1)$ denotes the wavelength conversion degree. Note that the cases of $d = 0$ and $d = W - 1$ correspond to no-wavelength conversion and full-range wavelength conversion, respectively.

Because there are no buffers in OBS nodes, the outgoing port with the W wavelengths can be considered as a multi-server retrial queueing system without waiting room. Since each wavelength is either in busy state or idle state, we need 2^W states to describe how the wavelength conversion technique works at a burst arrival epoch. In order to reduce the computational complexity, we assume that the probability that an incoming burst occupies an idle wavelength depends only on the number of busy wavelengths upon arrival. We then define q_j as the probability that an incoming burst who finds j $(j = 0, 1, \ldots, W)$ wavelengths busy upon its arrival occupies an available wavelength. The detailed computation of q_j is described in the next subsection.

We consider the worst retransmission case in which all IP packets contained in a burst are transmitted by TCP. In other words, IP packets discarded by burst segmentation are retransmitted at transport protocol level. Recall that an incoming burst preempts the ongoing transmission of the preceding burst with probability $1 - q_j$. In this case, the IP packets contained in the segmented tail part of the preempted burst are retransmitted by their source hosts, which are likely to detect the loss of their own IP packets at the same

$N(t) \leq M$: Number of
Retransmitted Bursts

Bursts Waiting for Retransmission

Dropped Part

New Burst	
Arrival Rate	λ
Average Length	$1/\mu$

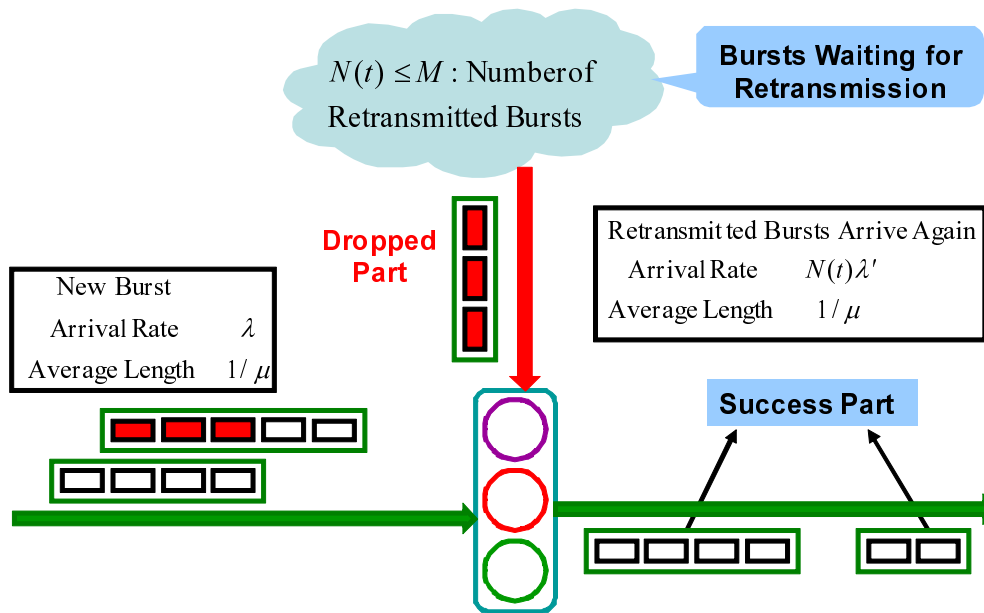| Retransmitted Bursts Arrive Again	
Arrival Rate	$N(t)\lambda'$
Average Length	$1/\mu$

Success Part

Figure 2: Analysis model

time. Then those lost packets may be retransmitted at the same time and are likely to be aggregated into the same burst at the OBS ingress-edge node. Therefore, we assume that the segmented tail part of the burst itself is retransmitted as a retransmitted burst at a later time. We also assume that when there are n retransmitted bursts, the retransmitted bursts arrive to the OBS node according to a Poisson process with rate $n\lambda'$. Suppose that the number of retransmitted bursts is limited to be no more than M. Finally we assume that transmission times of retransmitted bursts are i.i.d. according to an exponential distribution with rate μ'.

Under the above assumptions, the transmission service rate of retransmitted bursts is equal to that of original bursts, i.e., $\mu' = \mu$. This is justified as follows. Let us suppose an original burst having never been preempted is in transmission. Note that bursts arrive at the node according to a Poisson process, whose rate depends on the number of retransmissions in the network. Due to conditional PASTA (Poisson Arrivals See Time Averages) [8], the remaining service time seen by an arriving burst follows the same exponential distribution as the original service time. Thus we have $\mu' = \mu$. Figure 2 illustrates our analysis model.

3.2. Probability of success in idle server selection

This subsection discusses the probability q_j $(j = 0, 1, \ldots, W)$ that an arriving burst succeeds in being assigned to an idle wavelength. Recall here that q_j is the conditional probability that an arbitrary incoming burst occupies an idle wavelength in conversion range of the allocated wavelength, given that j wavelengths are busy upon its arrival. We assume that arriving bursts are uniformly assigned to W wavelengths. Thus an arbitrary incoming burst is allocated to w_l $(l = 1, 2, \ldots, W)$ with probability $1/W$. Given that j wavelengths are busy, the conditional probability that a wavelength arbitrarily chosen from among W wavelengths is busy is assumed to equal j/W. Note that a burst arriving at an incoming wavelength w_l $(l = 1, 2, \ldots, W)$ can only be converted onto outgoing wavelength $w_k \in \mathcal{W}_l$, where $\mathcal{W}_l$ is given in (3.1). The number h_l of the wavelengths in $\mathcal{W}_l$ $(l = 1, 2, \ldots, W)$ is given by
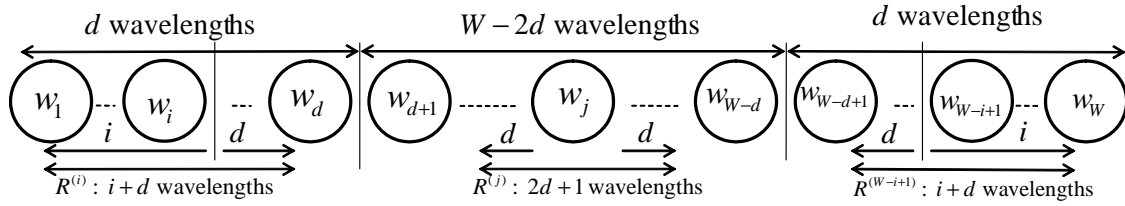
Figure 3: Conversion range

$$
h_l = \begin{cases} \min(l+d, W), & 1 \le l \le r, \\ \min(W-l+1+d, W), & W-r < l \le W, \\ \min(2d+1, W), & \text{otherwise}, \end{cases} \tag{3.2}
$$

where $r = \min(d, \lfloor W/2 \rfloor)$ (see Figure 3). Let $\bar{q}_j^{(l)}$ ($l = 1, 2, \ldots, W$) denote the probability that a burst originally allocated to w_l cannot find any idle wavelength in $\mathcal{W}_l$, given that j wavelengths are busy. We then have

$$
q_j = 1 - \sum_{l=1}^{W} \frac{1}{W} \cdot \bar{q}_j^{(l)}, \qquad j = 0, 1, \ldots, W. \tag{3.3}
$$

It follows from the above assumptions that $\bar{q}_j^{(l)}$ is equal to the probability that the j busy wavelengths include all the wavelengths of $\mathcal{W}_l$, i.e.,

$$
\bar{q}_j^{(l)} = \begin{cases} \binom{W-h_l}{j-h_l} / \binom{W}{j}, & h_l \le j \le W, \\ 0, & 0 \le j < h_l, \end{cases} \tag{3.4}
$$

where $\binom{n}{k} = 0$ for $n < k$.

4. Analysis of the Model

In this section, we first derive the system of linear equations of the steady state probabilities for the queueing model described in the previous section. Next, we obtain the following performance measures: the average number of busy wavelengths, the average number of retransmitted bursts, the contention probability and the average output burst size.

4.1. Steady state probabilities

Let $N(t)$ ($t \ge 0$) and $S(t)$ ($t \ge 0$) denote the number of retransmitted bursts and the number of busy wavelengths at time t, respectively. Note that $0 \le N(t) \le M$ and $0 \le S(t) \le W$ due to the assumption made in the previous section. Note also that arrivals of original bursts and those of retransmitted bursts follow Poisson processes with constant rate λ and state-dependent rate $\lambda' N(t)$, respectively. Then $(N(t), S(t))$ forms a bivariate Markov chain. We define $\boldsymbol{\pi}_i(t)$ ($t \ge 0$, $i = 0, 1, \ldots, M$) as a $1 \times (W+1)$ vector whose jth ($j = 0, 1, \ldots, W$) element $\pi_{i,j}(t)$ represents $\Pr[N(t) = i, S(t) = j]$. The Kolmogorov forward differential equations for $\{(N(t), S(t)); t \ge 0\}$ are given as follows: for $i = 0, 1, \ldots, M-1$,

$$
\frac{d}{dt}\pi_{i,0}(t) = -\pi_{i,0}(t)(\lambda + i\lambda' q_0) + \pi_{i,1}(t)\mu, \tag{4.1}
$$

$$\frac{d}{dt}\pi_{i,j}(t) = -\pi_{i,j}(t)\left(\lambda + j\mu + i\lambda'q_j\right) + \pi_{i,j-1}(t)\lambda q_{j-1} + \pi_{i-1,j}(t)\lambda(1-q_j),$$
$$+ \pi_{i,j+1}(t)(j+1)\mu + \pi_{i+1,j-1}(t)(i+1)\lambda'q_{j-1}, \quad j = 0, 1, \ldots, W-1, \quad (4.2)$$

$$\frac{d}{dt}\pi_{i,W}(t) = -\pi_{i,W}(t)(\lambda + W\mu) + \pi_{i,W-1}(t)\lambda q_{W-1} + \pi_{i-1,W}(t)\lambda$$
$$+ \pi_{i+1,W-1}(t)(i+1)\lambda'q_{W-1}, \quad (4.3)$$

and for $i = M$,

$$\frac{d}{dt}\pi_{M,0}(t) = -\pi_{M,0}(t)(\lambda + M\lambda'q_0) + \pi_{M,1}(t)\mu, \quad (4.4)$$

$$\frac{d}{dt}\pi_{M,j}(t) = -\pi_{M,j}(t)\left(\lambda q_j + j\mu + M\lambda'q_j\right) + \pi_{M,j-1}(t)\lambda q_{j-1}$$
$$+ \pi_{M,j+1}(t)(j+1)\mu + \pi_{M-1,j}(t)\lambda(1-q_j), \quad j = 0, 1, \ldots, W-1, \quad (4.5)$$

$$\frac{d}{dt}\pi_{M,W}(t) = -\pi_{M,W}(t)(\lambda q_W + W\mu + M\lambda'q_W) + \pi_{M,W-1}(t)\lambda q_{W-1}$$
$$+ \pi_{M-1,W}(t)\lambda(1-q_W). \quad (4.6)$$

To rewrite (4.1)–(4.6), we define $\boldsymbol{A}^+$, $\boldsymbol{A}_i^-$ and $\boldsymbol{A}_i$ $(i = 0, 1, \ldots, M)$ as

$$\boldsymbol{A}^+ = \begin{bmatrix} \lambda(1-q_0) & 0 & \cdots & 0 & 0 \\ 0 & \lambda(1-q_1) & \cdots & 0 & 0 \\ \vdots & \vdots & \ddots & \vdots & \vdots \\ 0 & 0 & \cdots & \lambda(1-q_{W-1}) & 0 \\ 0 & 0 & \cdots & 0 & \lambda(1-q_W) \end{bmatrix},$$

$$\boldsymbol{A}_i^- = \begin{bmatrix} 0 & i\lambda'q_0 & 0 & 0 & \cdots & 0 \\ 0 & 0 & i\lambda'q_1 & 0 & \cdots & 0 \\ 0 & 0 & 0 & \ddots & \ddots & 0 \\ \vdots & \vdots & \vdots & \ddots & i\lambda'q_{W-2} & 0 \\ 0 & 0 & 0 & \ddots & 0 & i\lambda'q_{W-1} \\ 0 & 0 & 0 & \cdots & 0 & 0 \end{bmatrix}, \quad i = 1, 2, \ldots, M,$$

and

$$\boldsymbol{A}_i = \begin{bmatrix} b_0^{(i)} & a_1^{(i)} & 0 & \cdots & 0 & 0 \\ c_0^{(i)} & b_1^{(i)} & a_2^{(i)} & \cdots & 0 & 0 \\ 0 & c_1^{(i)} & b_2^{(i)} & \cdots & 0 & 0 \\ 0 & 0 & c_2^{(i)} & \ddots & a_{W-1}^{(i)} & 0 \\ 0 & 0 & 0 & \ddots & b_{W-1}^{(i)} & a_W^{(i)} \\ 0 & 0 & 0 & \cdots & c_{W-1}^{(i)} & b_W^{(i)} \end{bmatrix}, \quad i = 0, 1, \ldots, M,$$

respectively, where

$$b_0^{(i)} = -(\lambda + i\lambda'q_0), \quad b_j^{(i)} = -(\lambda(q_j\delta_{i,M} - \delta_{i,M} + 1) + j\mu + i\lambda'q_j)$$
$$(j = 0, 1, \ldots, W),$$

$$a_j^{(i)} = \lambda q_{j-1} \quad (j = 1, \ldots, W), \qquad c_j^{(i)} = (j+1)\mu \quad (j = 0, 1, \ldots W-1).$$

We then rewrite (4.1)–(4.6) as

$$\frac{d}{dt}\boldsymbol{\pi}_k(t) = \boldsymbol{\pi}_{k-1}(t)\boldsymbol{A}^+ + \boldsymbol{\pi}_k(t)\boldsymbol{A}_k + \boldsymbol{\pi}_{k+1}(t)\boldsymbol{A}_{k+1}^-, \qquad k = 0, 1, \ldots, M-1, \qquad (4.7)$$

$$\frac{d}{dt}\boldsymbol{\pi}_M(t) = \boldsymbol{\pi}_{M-1}(t)\boldsymbol{A}^+ + \boldsymbol{\pi}_M(t)\boldsymbol{A}_M, \qquad (4.8)$$

where $\boldsymbol{\pi}_{-1}(t) = \boldsymbol{0}$ for all $t \geq 0$. Let $\boldsymbol{\pi} = (\boldsymbol{\pi}_0, \boldsymbol{\pi}_1, \ldots, \boldsymbol{\pi}_M)$, where $\boldsymbol{\pi}_i = \lim_{t\to\infty} \boldsymbol{\pi}_i(t)$. It then follows from (4.7) and (4.8) that $\boldsymbol{\pi}$ is a probability vector satisfying $\boldsymbol{\pi}\boldsymbol{Q} = \boldsymbol{0}$, where

$$\boldsymbol{Q} = \begin{bmatrix} \boldsymbol{A}_0 & \boldsymbol{A}^+ & \boldsymbol{O} & \cdots & \boldsymbol{O} & \boldsymbol{O} & \boldsymbol{O} \\ \boldsymbol{A}_1^- & \boldsymbol{A}_1 & \boldsymbol{A}^+ & \cdots & \boldsymbol{O} & \boldsymbol{O} & \boldsymbol{O} \\ \boldsymbol{O} & \boldsymbol{A}_2^- & \boldsymbol{A}_2 & \ddots & \boldsymbol{O} & \boldsymbol{O} & \boldsymbol{O} \\ \vdots & \vdots & \ddots & \ddots & \ddots & \vdots & \vdots \\ \boldsymbol{O} & \boldsymbol{O} & \boldsymbol{O} & \cdots & \boldsymbol{A}_{M-1}^- & \boldsymbol{A}_{M-1} & \boldsymbol{A}^+ \\ \boldsymbol{O} & \boldsymbol{O} & \boldsymbol{O} & \cdots & \boldsymbol{O} & \boldsymbol{A}_M^- & \boldsymbol{A}_M \end{bmatrix}.$$

Note that $\boldsymbol{\pi}$ can be regarded as the stationary distribution vector of a finite quasi-birth-and-death process, for which some efficient algorithms have been proposed, e.g. the folding algorithm [20]. However, because block matrices $\boldsymbol{A}_i$ $(i = 0, 1, \ldots, M)$, $\boldsymbol{A}_i^-$ $(i = 1, 2, \ldots, M)$ and $\boldsymbol{A}^+$ in $\boldsymbol{Q}$ are extremely sparse, we compute $\boldsymbol{\pi}$ by a solver called *lusolve* in Scilab [15], which was developed for solving sparse systems of linear equations. Throughout some numerical examples, we confirmed that solver lusolve is more efficient than the folding algorithm, especially when the size of $\boldsymbol{Q}$ is large.

4.2. Performance measures

In this subsection, we discuss some performance measures of the stationary system. Let N and S denote generic random variables for $N(t)$ and $S(t)$, respectively, in steady state. Let $\pi_j^{(S)}$ $(j = 0, 1, \ldots, W)$ denote the marginal probability that there are j busy wavelengths, i.e., $\Pr[S = j]$. Let $\pi_i^{(N)}$ denote the marginal probability that there are i retransmitted bursts, i.e., $\Pr[N = i]$. Noting $\pi_{i,j} = \Pr[N = i, S = j]$, we have

$$\pi_j^{(S)} = \sum_{i=0}^M \pi_{i,j}, \qquad j = 0, 1, \ldots, W,$$

$$\pi_i^{(N)} = \sum_{j=0}^W \pi_{i,j}, \qquad i = 0, 1, \ldots, M.$$

Thus the average number of busy wavelengths and the average number of bursts in retransmission are given by

$$\mathrm{E}[S] = \sum_{j=0}^W j \pi_j^{(S)}, \qquad \mathrm{E}[N] = \sum_{i=0}^M i \pi_i^{(N)},$$

respectively.

Let P_{cont} denote the contention probability of an arbitrary arriving burst. Note that an arriving burst who finds j wavelengths being busy upon its arrival preempts the transmission of a burst with probability $1 - q_j$. We then have

$$P_{cont} = \sum_{j=0}^W (1 - q_j) \Pr(S = j) = \sum_{j=0}^W (1 - q_j) \pi_j^{(S)}.$$

Finally, we derive the average output burst size. Let L denote a generic random variable for output burst sizes. We then have

$$
\begin{aligned}
\mathrm{E}[L] &= \sum_{i=0}^{M}\sum_{j=1}^{W} \Pr((N,S)=(i,j) \mid S \neq 0)\mathrm{E}[L \mid N=i, S=j>0] \\
&= \sum_{i=0}^{M}\sum_{j=1}^{W} \frac{\pi_{i,j}}{1-\pi_0^{(S)}} \cdot \mathrm{E}[L \mid N=i, S=j>0],
\end{aligned} \tag{4.9}
$$

where we use $\Pr[S \neq 0] = 1 - \pi_0^{(S)}$ in the second equality. To calculate $\mathrm{E}[L \mid N=i, S=j>0]$, we consider the case that there are i $(i=0,1,\ldots,M)$ retransmitted bursts and j $(j=1,2,\ldots,W)$ busy wavelengths. Owing to the assumptions in section 3, an incoming burst occupies a busy wavelength with probability $1-q_j$ and therefore arrivals of bursts to one of j busy wavelengths form a Poisson process with rate $(\lambda+i\lambda')(1-q_j)/j$. Thus we have

$$
\mathrm{E}[L \mid N=i, S=j>0] = \frac{1}{\mu + (\lambda+i\lambda')(1-q_j)/j},
$$

from which and (4.9) it follows that

$$
\mathrm{E}[L] = \sum_{i=0}^{M}\sum_{j=1}^{W} \frac{\pi_{i,j}}{1-\pi_0^{(S)}} \frac{1}{\mu + (\lambda+i\lambda')(1-q_j)/j}. \tag{4.10}
$$

5. Numerical Examples

In this section, we show some numerical examples. Simulation was also performed to validate the analysis. In the simulation model, an arriving burst finding its allocated wavelength in busy state attempts to use another wavelength within its conversion range. If there are multiple idle wavelengths in the conversion range, the burst will be forwarded to one of them randomly. Otherwise, it preempts the ongoing burst transmission on the allocated wavelength. The retransmitted burst is retransmitted after an exponentially distributed time with mean $1/\lambda'$. We set $M=1000$, and the mean transmission time of an original burst, $1/\mu$, equal to 10.0 ms. Note that this corresponds to the case that the transmission speed of an outgoing wavelength equals 10 Gbps and the mean number of IP packets with size of 1,250 bytes in a burst is 10,000. We define the traffic intensity as $\rho = \lambda/(W\mu)$. We also assume that $\lambda' = 0.1$ which corresponds to the case that the average retransmission timeout period (RTO) is 100 ms. We consider two cases of $W=8$ and 32.

Figures 4 and 5 show the average number of busy wavelengths $\mathrm{E}[S]$ against the traffic intensity for $W=8$ and 32, respectively. In each figure, the following four cases are plotted: no wavelength conversion $(d=0)$, limited wavelength conversion $(d=1,2)$ and full wavelength conversion. We observe from Figure 4 that the simulation results fit the analytical results precisely and that $\mathrm{E}[S]$'s for the four cases are almost the same when ρ is small. When the traffic intensity is large, the average number of busy wavelengths increases monotonically. When the traffic intensity gets greater than 0.8, the analytical results draw away from simulation. This is because in the analysis model, we assume that the arrival of retransmitted bursts follows a Poisson process with a rate proportional to the number of retransmitted bursts. However, because an incoming burst may preempt the transmission of the ongoing burst, it may influence the future arrival of bursts. Figure 5 shows the average number of busy wavelengths against the traffic intensity when the number
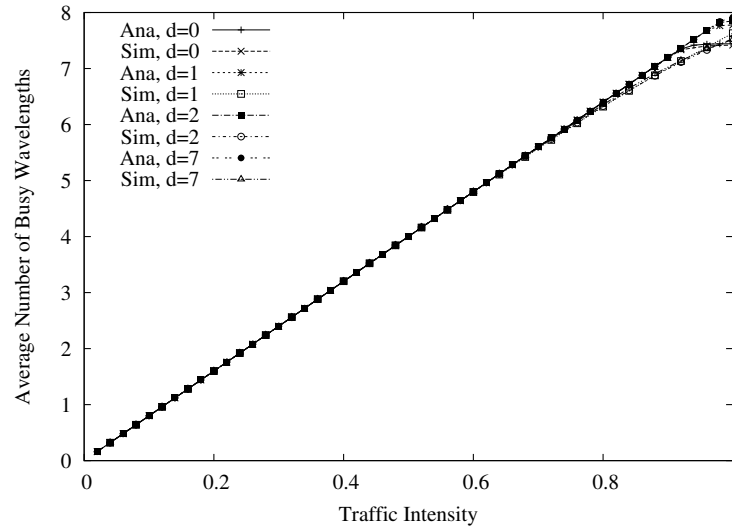
Figure 4: Average number of busy wavelengths E[S] against ρ ($W = 8$)

of wavelengths is $W = 32$. We observe that the trends of E[S]'s in Figure 5 are similar to those in Figure 4. Note that the analytical results exhibit a good agreement with simulation results for $0 < \rho < 0.8$. This suggests that our analysis is effective when the traffic intensity is in the range of $(0, 0.8)$. In what follows, we investigate the performance of the system for $0 < \rho < 0.8$.

Figures 6 and 7 show the contention probabilities against the traffic intensity for the cases $W = 8$ and 32, respectively. It is observed from Figures 6 and 7 that the analytical results agree well with the simulation results for $d = 0$ (no-wavelength conversion) and $W - 1$ (full-range wavelength conversion). In these special cases, we have $q_j = 1 - j/W$ ($j = 0, 1, \ldots, W$) for $d = 0$ and $q_j = 1 - \delta_{j,W}$ ($j = 0, 1, \ldots, W$) for $d = W - 1$, where $\delta_{i,j}$ is the Kronecker's δ. Note that in both the cases, the performance measures can be calculated accurately. In the case of limited range wavelength conversion, we assumed that the states of all the wavelengths are independent. However, the states of the wavelengths in the same
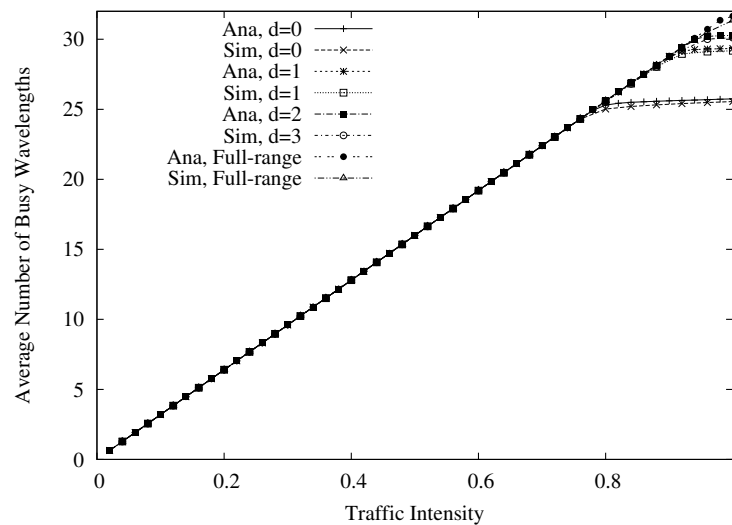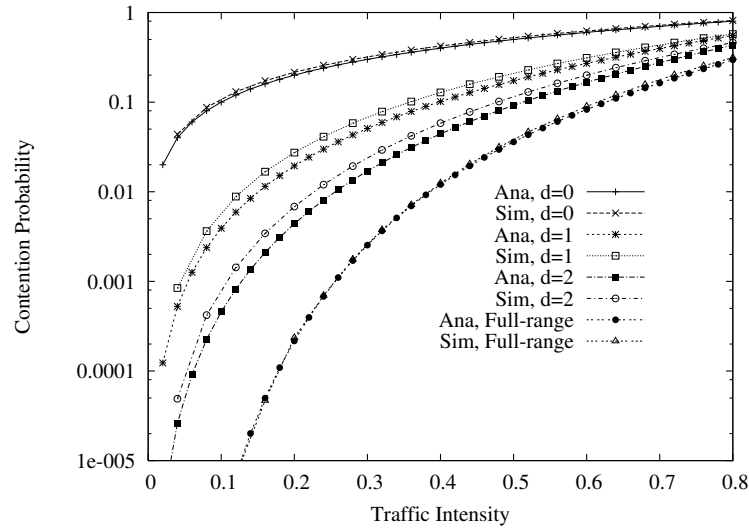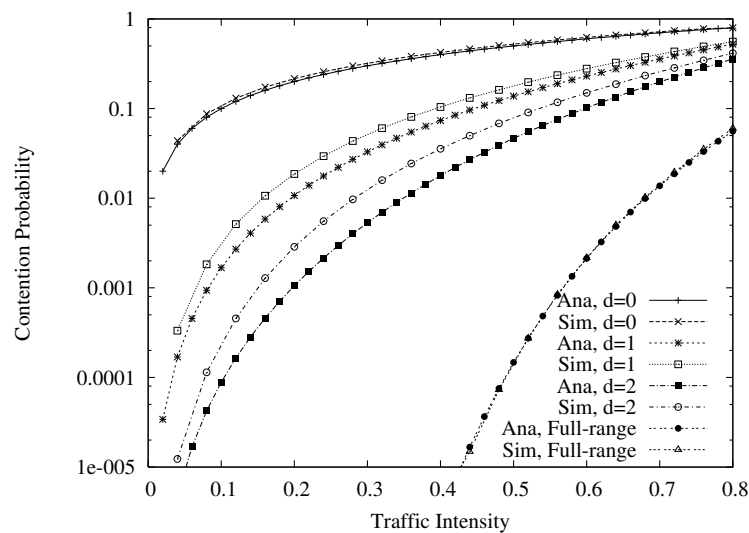

Figure 5: Average number of busy wavelengths E[S] against ρ ($W = 32$)

Figure 6: Contention probability P_{cont} against ρ ($W = 8$)

Figure 7: Contention probability P_{cont} against ρ ($W = 32$)

conversion range of a wavelength depend on each other since a burst originally allocated to a wavelength might be forwarded to another wavelength in a conversion range. Therefore, when a wavelength is in busy state, each of the neighboring wavelengths in its conversion range is in busy state with a higher probability than that derived under the independence assumption. We observe that the contention probability increases as the traffic intensity gets larger, as expected. We also observe that the contention probability decreases with the increase in the wavelength conversion degree d. This is because an incoming burst finding its originally allocated wavelength busy is more likely to find an idle wavelength in a larger conversion range. Note that the contention probability significantly decreases even for $d = 1$. This suggests that the contention probability can be notably diminished by the introduction of wavelength conversion even with a small wavelength conversion degree d.

Figures 8 and 9 illustrate the contention probability P_{cont} against d for the cases of $W = 8$ and 32, respectively, keeping ρ constant ($\rho = 0.4$, 0.6 and 0.8). It is observed
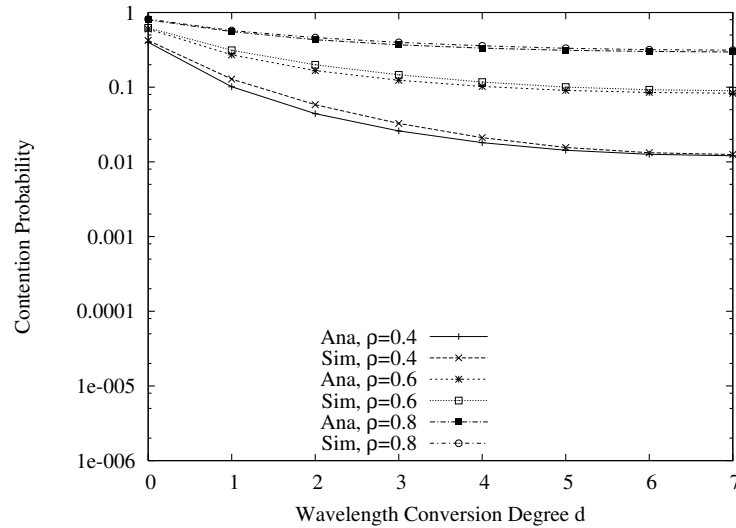
Figure 8: Contention probability P_{cont} against d ($W = 8$)

from both the figures that the contention probabilities decrease as d increases. It is also observed that in cases of low traffic intensity, the effectiveness of wavelength conversion is remarkable. In Figure 8, the contention probability dramatically decreases in a small wavelength conversion degree d, while it remains constant as d approaches to $W - 1$. In Figure 9, the contention probability exhibits the same tendency as that in Figure 8. Note that the contention probability for $W = 32$ is greatly improved by the increase in d in comparison with that for $W = 8$. This result implies that limited wavelength conversion is significantly effective in decreasing the contention probability for the OBS network in which a large number of wavelengths are multiplexed in an optical fiber.

Figures 10 and 11 illustrate the average number of retransmitted bursts E[N], against the traffic intensity ρ. In both figures, E[N] increases as the traffic intensity increases, as expected. We also observe that E[N] for $d = 0$ decreases significantly with the increase in d. This implies that limited wavelength conversion can significantly decrease the number of
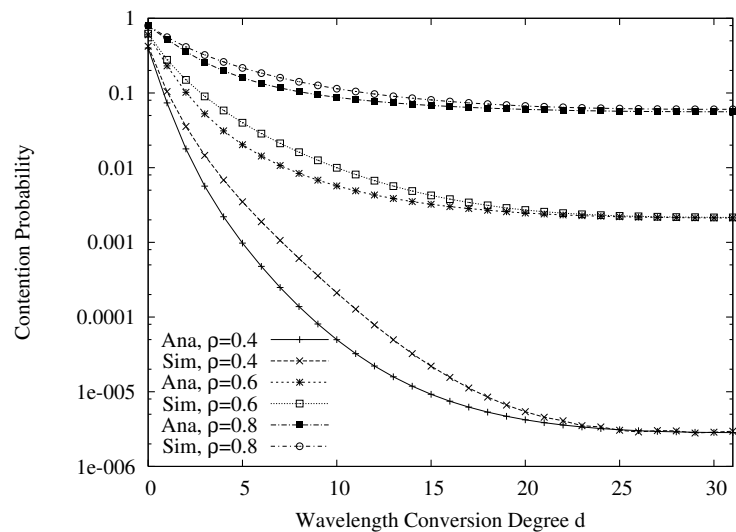

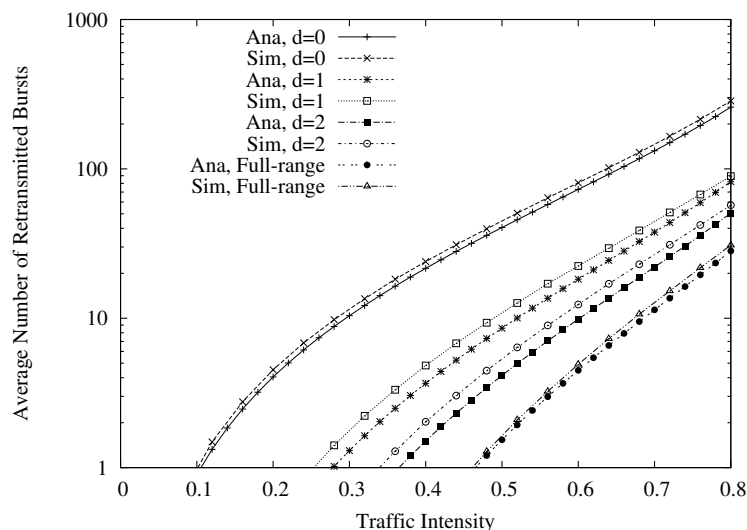Figure 9: Contention probability P_{cont} against d ($W = 32$)

Figure 10: The average number of retransmitted bursts E[N] against ρ ($W = 8$)

retransmitted bursts. It is also observed that a wider conversion range results in a smaller number of retransmitted bursts and that the number of retransmitted bursts for the cases of full-range wavelength conversion is much smaller than that for the cases of small range wavelength conversion. This implies that the wavelength conversion technique significantly reduces the number of retransmitted bursts.

Next, we consider how the retransmission rate affects the performance of the OBS network with burst segmentation and limited wavelength conversion. Figure 12 represents the contention probability against the retransmission rate λ' for $\rho = 0.5$. Here, the retransmission rate λ' is varied from 10^{-2} to 10^{-1}. This is equivalent to changing the average retransmission timeout period (RTO) from 1000 ms to 100 ms. We observe that the contention probability remains constant and hence it is almost insensitive to the retransmission rate. This is because the number of retransmitted bursts which arrive at the system during a unit time does not change for different values of the retransmission timeout period. As a
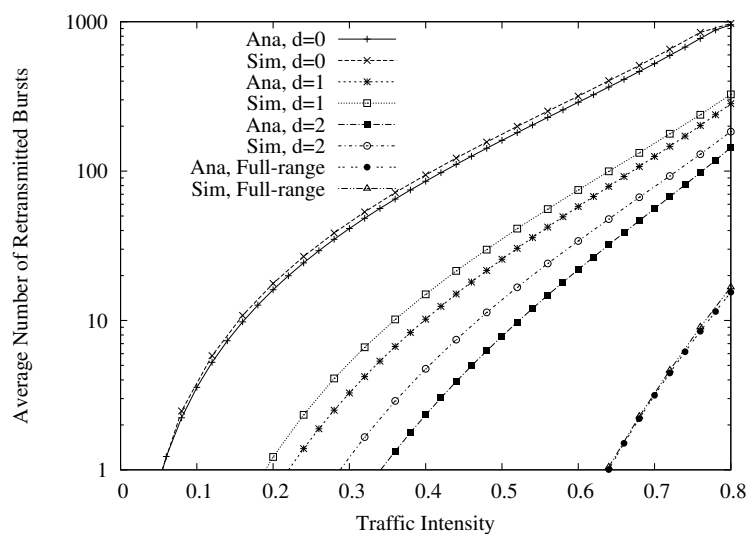

Figure 11: The average number of retransmitted bursts E[N] against ρ ($W = 32$)
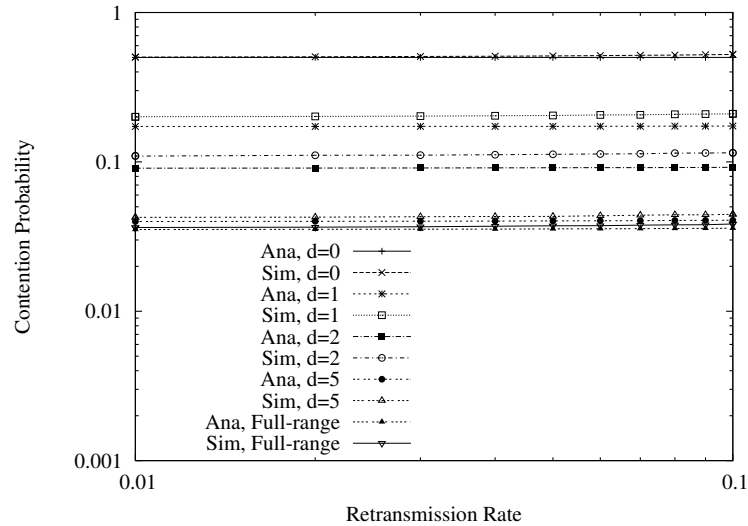
Figure 12: Contention probability P_{cont} against λ' ($\rho = 0.5$)

result, the contention probability does not change with λ'. Figure 13 shows the number of retransmitted bursts against the retransmission rate. We observe that the average number of retransmitted bursts $E[N]$ decreases as λ' increases. The reason for this is that the number of retransmitted bursts arriving in a unit time is almost insensitive to the retransmission timeout and equals the product of λ' and the number of retransmitted bursts. It is also observed that $E[N]$ for $d = 0$ is the largest, while that for $d = 7$ (full-range wavelength conversion) is the smallest. The reason is the same as that for Figure 10.

Figures 14 and 15 show the average output burst size against the traffic intensity for cases of $W = 8$ and 32, respectively. It is observed from both figures that the average output burst size gets smaller with the increase in the traffic intensity. This is because when the traffic intensity is high, burst segmentation occurs frequently, resulting in a small average output burst size. We also observe that in the case of $d = 0$, the analytical results agree well with the simulation. In the cases of $d = 1$ and 2, however, there exists a discrepancy
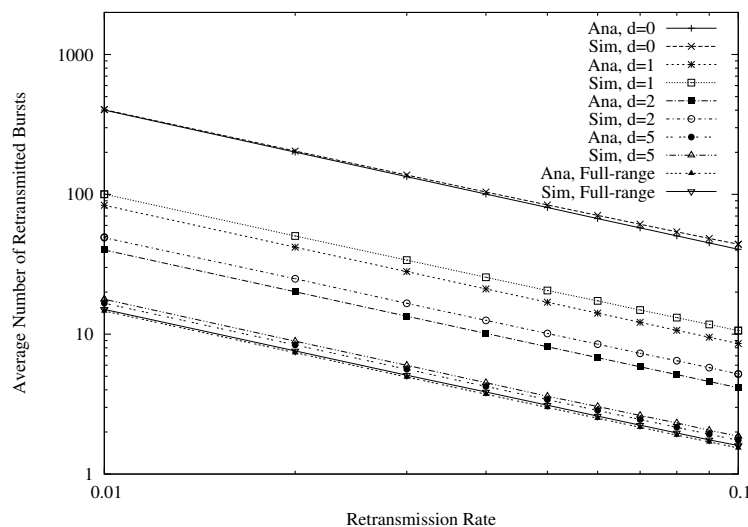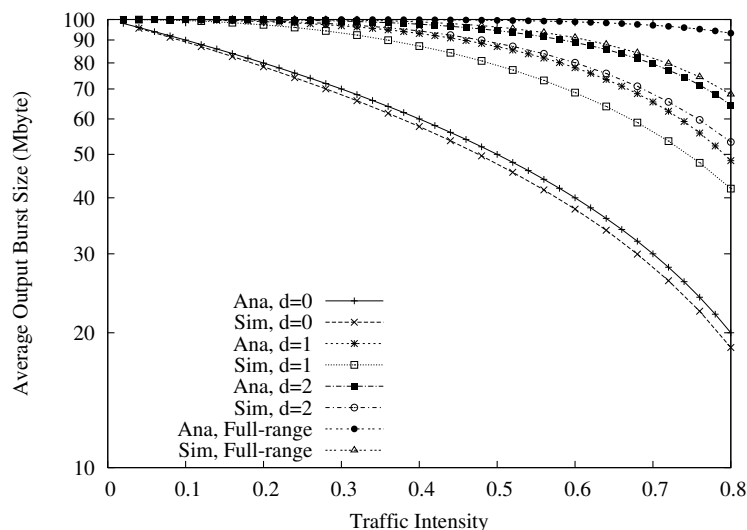

Figure 13: Average number of retransmitted bursts $E[N]$ against λ' ($\rho = 0.5$)

Figure 14: Average output burst size E[L] against ρ ($W = 8$)

between them. Note that for the OBS network with wavelength conversion, bursts requesting some wavelength are not only those originally allocated to the wavelength but also those converted from the other wavelengths in its conversion range. Therefore, the utilization of a wavelength with a smaller conversion range gets smaller. In the analysis model, however, we assumed that the arriving bursts are uniformly distributed. This causes a discrepancy between analysis and simulation results. It is also observed that the discrepancy between analysis and simulation for $W = 32$ (Figure 15) is smaller than that for $W = 8$ (Figure 14). This implies that the analysis model works well when the wavelength conversion degree d is relatively small compared to the number of wavelengths.
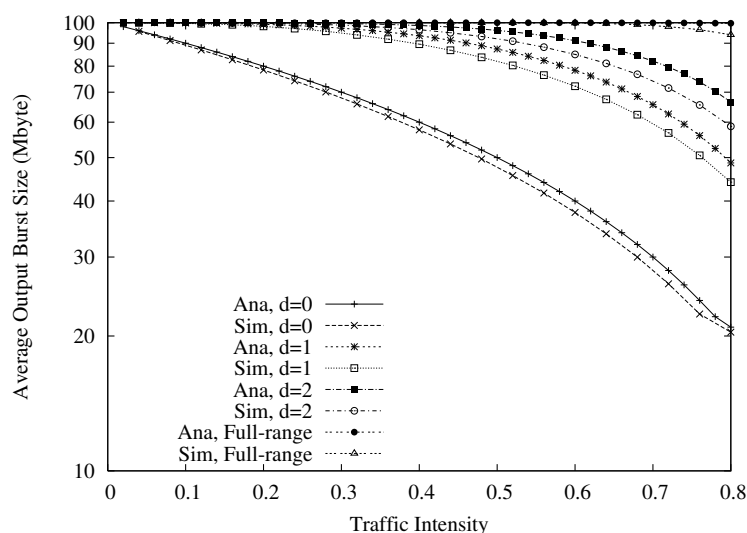
Figure 15: Average output burst size E[L] against ρ ($W = 32$)

6. Conclusion

In this paper, we have analyzed the performance of the OBS network with burst segmentation, wavelength conversion and upper-layer retransmission. To model the system, we have

developed a multi-server queueing system with random server selection which covers the three special cases: no wavelength conversion, limited wavelength conversion and full wavelength conversion. We have analyzed the model using a bivariate Markov chain to derive the average number of busy wavelengths, the contention probability, the average number of retransmitted bursts and the average output burst size.

The numerical examples have shown that the analytical results agree well with the simulation results when the traffic intensity is moderate. As for retransmission, the contention probability is almost insensitive to the retransmission rate, while the average number of retransmitted bursts is greatly affected by the retransmission rate. The wavelength conversion is effective to alleviate the contention among bursts at a low traffic intensity, however, it is less effective at a high traffic intensity. More precisely, OBS networks with a small wavelength conversion degree cause a large number of retransmitted bursts, a high contention probability, and a small average output burst size in comparison with those with a large wavelength conversion degree. In addition, the contention probability becomes insensitive as the wavelength conversion degree gets close to the number of wavelengths.

References

[1] T. Battestilli and H. Perros: An introduction to optical burst switching. *IEEE Communications Magazine*, **41** (2003), S10–S15.

[2] F. Callegati: Optical buffers for variable length packets. *IEEE Communications Letters*, **4** (2000), 292–294.

[3] Y. Chen, C. Qiao and S. Yu: Optical burst switching (OBS): A new area in optical networking research. *IEEE Network Magazine*, **18** (2004), 16–23.

[4] Y. Chen, H. Wu, D. Xu and C. Qiao: Performance analysis of optical burst switched node with deflection routing. *Proceedings of IEEE International Conference on Communications 2003* (2003), 1355–1359.

[5] J.Y. Choi, J.S. Choi and M. Kang: Performance analysis of optical-level buffered optical burst switching node with retransmission technique. *IEICE Transactions on Information and Systems*, **E89-D** (2006), 452–458.

[6] A. Detti, V. Eramo and M. Listanti: Performance evaluation of a new technique for IP support in a WDM optical network: optical composite burst switching (OCBS). *Journal of Lightwave Technology*, **20** (2002), 154–165.

[7] G.I. Falin and J.G.C. Templeton: *Retrial Queues* (Chapman & Hall, London, 1997).

[8] D. König and V. Schmidt: Extended and conditional versions of the PASTA property. *Advances in Applied Probability*, **22** (1990), 510–512.

[9] M. Neuts, H. L. Vu and M. Zukerman: Insight into the benefit of burst segmentation in optical burst switching. *Proceedings of International Conference on Optical Internet and Photonics in Switching 2002* (2002), 126–128.

[10] M. Neuts, H.L. Vu and M. Zukerman: Performance analysis of optical composite burst switching. *IEEE Communications Letters*, **6** (2002), 346–348.

[11] T. Phung-Duc, H. Masuyama, S. Kasahara and Y. Takahashi: Burst segmentation with retransmission of upper-layer and its effect on wavelength utilization for optical burst switched networks. *Proceedings of The First International Conference on Communications and Electronics 2006* (2006), 35–40.

[12] C. Qiao and M. Yoo: Optical burst switching (OBS) – a new paradigm for an optical internet. *Journal of High Speed Networks*, **1** (1999), 69–84.

[13] C. Qiao and M. Yoo: Choices, features and issues in optical burst switching. *Optical Networks*, **1** (2000), 36–44.

[14] Z. Rosberg, A. Zalesky, H.L. Vu and M. Zukerman: Analysis of OBS networks with limited wavelength conversion. *IEEE/ACM Transactions on Networking*, **14** (2006), 1118–1127.

[15] Scilab: Scilab Home Page, *http://www.scilab.org*.

[16] J.S. Turner: Terabit burst switching. *Journal of High Speed Networks*, **8** (1999), 3–16.

[17] S. Verma, H. Chaskar and R. Ravikanth: Optical burst switching: a viable solution for terabit IP backbone. *IEEE Network*, **14** (2000), 48–53.

[18] V.M. Vokkarane, J.P. Jue and S. Sitaraman: Burst segmentation: an approach for reducing packet loss in optical burst switched networks. *Proceedings of IEEE International Conference on Communications 2002* (2002), 2673–2677.

[19] V.M. Vokkarane and J.P. Jue: Prioritized burst segmentation and composite burst-assembly techniques for QoS support in optical burst-switched networks. *IEEE Journal on Selected Areas in Communications*, **21** (2003), 1198–1209.

[20] J. Ye and S.Q. Li: Folding algorithm: a computational method for finite QBD process with level dependent transitions. *IEEE Transactions on Communications*, **42** (1994), 625–639.

[21] Q. Zhang, V.M. Vokkarane, Y. Wang and J.P. Jue: Analysis of TCP over optical burst-switched networks with burst retransmission. *Proceedings of IEEE Global Communications Conference 2005*, **24** (2005), 1977–1982.

Tuan Phung-Duc
Department of Systems Science
Graduate School of Informatics
Kyoto University, Yoshida-Honmachi
Sakyo-ku, Kyoto 606-8501, Japan
E-mail: `tuan@sys.i.kyoto-u.ac.jp`